Adsorption Removal of Dyes from Single and Binary Solutions Using a Cellulose-based Bioadsorbent

Lin Liu,[†,‡] Zhang Yun Gao,[†] Xiu Ping Su,[†] Xing Chen,[†] Li Jiang,[†] and Ju Ming Yao*[,†,‡]

[†]The Key Laboratory of Advanced Textile Materials and Manufacturing Technology of Ministry of Education, College of Materials and Textiles, Zhejiang Sci-Tech University, Hangzhou 310018, China

[‡]National Engineering Lab of Textile Fiber Materials & Processing Technology, Hangzhou 310018, China

S *Supporting Information*

ABSTRACT: A high efficiency and eco-friendly porous cellulose-based bioadsorbent was synthesized by grafting acrylic acid and acrylamide to remove anionic dye acid blue 93 (AB93) and cationic dye methylene blue (MB) from single and binary dye solutions. The effects of initial dye concentration, bioadsorbent dosage, contact time, solution pH value, temperature, ionic strength and surfactant content on the adsorption capacity of the bioadsorbent were investigated. The maximum adsorption capacities of the bioadsorbent for both AB93 and MB were 1372 mg g^{-1} at an initial concentration of 2500 mg L^{-1}. The conditions-dependent adsorption characteristics of the bioadsorbent indicated a high efficiency of dyes removal. The appropriate isotherm model for the equilibrium process was the Freundlich, and the kinetic studies revealed that the adsorption of AB93 and MB followed the pseudo-second-order kinetic models. The adsorbent behaviors were dominated by the electrostatic interactions between the bioadsorbents and the dye molecules. Moreover, the recyclability experiments showed that the bioadsorbent could be reused for at least three cycles with stable adsorption capacity even in complex systems containing binary-dyes, salt, and surfactant. Thus, the cellulose-based bioadsorbent can be effectively used for the removal of dyes from industrial textile wastewater.

KEYWORDS: Cellulose-based bioadsorbent, adsorption, dye removal, dye auxiliary, recyclability

INTRODUCTION

Water pollution is an important environmental issue, and receives major worldwide concern.[1−3] Dyes discharged together with industrial textile wastewaters are main organic pollutants because they are highly visible and undesirable even at low concentrations in water.[4−6] More seriously, most organic dyes are toxic, nonbiodegradable, and even teratogenetic, carcinogenic, and mutagenic, which create the serious threats to human health and marine organisms.[7,8] Hence, the dyes must be efficiently removed from the discharged wastewater to solve the ecological, biological, and industrial problems.

In the process of dye removal from wastewaters, many treatment methods, including chemical precipitation,[9,10] ion exchange,[11,12] membrane filtration,[13,14] physical adsorption,[15,16] chemical oxidation/reduction,[17,18] and bioremoval,[19,20] have been developed. Among these, the adsorption technique is considered as a competitive method for treatment of dyestuff wastewater due to its easy handling, high efficiency, and economic feasibility.[21−23] The adsorbents with high capacity and high rate play a critical role in the adsorption removal of dye molecules. The activated carbon is a commercial adsorbent for eliminating pollutions from wastewater and air. However, the higher production cost, and regeneration difficulty of activated carbon limit its widespread use.[24−26] Thus, the

development of cheaper, eco-friendly, and more efficient adsorbent is a subject of intensive research.[27−32]
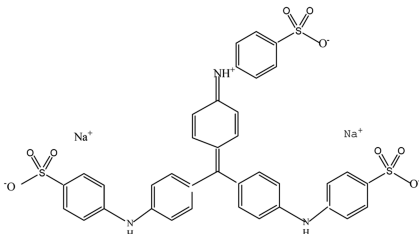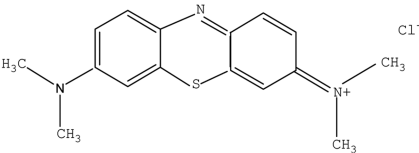
Cellulose is the most abundant natural polymer with good properties such as low cost, biodegradability, eco-friendly, and high stability to most organic solvents.[33,34] Moreover, the cellulose molecules have high density of hydroxyl groups, and can be modified with specific functional groups, such as carboxyl,[35] amino,[36] sulfo group,[37] and cyclodextrin,[38,39] to remove specific pollutants. The cellulose modified with multicarboxyl was reported to adsorb the cationic dyes in water.[35] The cellulose-based adsorbent modified with carboxyl and sulfo groups exhibited better adsorption ability and efficiency for crystal violet than those of native cellulose.[37] The surface quaternized cellulose nanofibrils were demonstrated to have the adsorption capacity for the anionic dyes.[40] The cellulose-graft-acrylic acid hydrogels were used to remove heavy metal ions, and revealed that the complexation between the metal ions and the carboxyl groups on the hydrogels was the main adsorption mechanism.[41] These reports demonstrated that the adsorption capacity of an adsorbent is determined not

Table 1. Chemical Structure and Some Properties of Acid Blue 93 and Methylene Blue

Dyes	Chemical formula	Molar mass (g mol^{-1})	λ_{max} (nm)	Electrical property
Acid Blue 93 (AB93)		799.80	664	Anionic
Methylene Blue (MB)		319.86	607	Cationic

only by the surface characteristics of the adsorbent but also by the properties of adsorbates.

In this study, we synthesized a novel three-dimensional porous cellulose-based bioadsorbent modified with acrylic acid and acrylamide for eliminating the pollutants from aqueous solution. Two organic dyes (acid blue 93 (AB93), methylene blue (MB)), and two auxiliaries (NaCl and SDS) were used as model pollutants to investigate the adsorption characteristics of cellulose-based bioadsorbent in complex systems. Acid blue 93 and methylene blue are anionic and cationic dyes, respectively, and their chemical structures and some properties are listed in Table 1. The main objective of this work is to investigate the simultaneous removal of both anionic and cationic dyes from the complex systems. Furthermore, the recyclability of the cellulose-based bioadsorbent was investigated. The results indicated that the cellulose-based bioadsorbent could be used as a desirable adsorbent for environmental remediation.

■ EXPERIMENTAL SECTION

Materials. Cellulose was obtained from mulberry branches by smashing into powders with size of ca. 100 mesh.[42] Acrylic acid (AA), acrylamide (AM), ammonium persulfate (APS), *N,N′*-methylenebis-(acrylamide) (MBA), ethanol, NaCl, sodium dodecyl sulfate (SDS), acid blue 93 (AB93) and methylene blue trihydrate (MB) were purchased from Sinopharm Chemical.

Synthesis of Bioadsorbent. Cellulose-based bioadsorbent was synthesized by graft copolymerization using mulberry branches as raw materials on the basis of our previous reports.[43,44] 2 g cellulose powders were dispersed into 50 mL deionized water to form a suspension solution. 2 mL of ammonium persulfate solution (0.1 g mL^{-1}) was added into the suspension solution under stirring for 15 min. Then 10 mL of aqueous solution containing acrylic acid (8 g), acrylamide (2 g), and *N,N′*-methylenebis(acrylamide) (0.06 g) was added into above reaction mixture. The polymerization reaction was performed at 70 °C for 2 h. The production was neutralized with sodium hydroxide solution, dehydrated with ethanol, and finally dried at 60 °C in a vacuum oven.

Structural Characterization. The surface morphology of the cellulose-based bioadsorbent was imaged using scanning electron microscopy (SEM, JEOL, JSM-5610, Japan) after sputtering with gold. The chemical structures of cellulose powders, bioadsorbent, and dyes

loaded bioadsorbent were characterized by Fourier transform infrared spectroscopy (FTIR, Nicolet 5700, Thermo Electron Corp., USA) ranging from 4000 to 400 cm^{-1}. The contents of carboxyl and amino groups per gram of bioadsorbent were determined using a titration method.[35,36] The surface ζ-potential of the bioadsorbent was measured using a Zetasizer Nano-ZS90 (Malvern, United Kingdom). The surface area of the bioadsorbent was measured using the Brunauer−Emmett−Teller (BET, 3H-2000PS1, BeiShiDe Instrument Technology Co. Ltd., China) method, and the sample was degassed at 50 °C prior to nitrogen adsorption measurement.

Water Absorbency of Bioadsorbent. The water absorbency of the bioadsorbent was measured in aqueous solution at various pH values. The bioadsorbents were weighed (W_0) and immersed in 500 mL of aqueous solution at 25 °C. At an interval time, the swollen bioadsorbents were taken out and weighed (W_t) after removing excess water with a filter paper. The water adsorption capacity was calculated from the following eq 1.

$$\text{water absorption (g g}^{-1}) = \frac{W_t - W_0}{W_0} \tag{1}$$

Adsorption of Dyes in Single System. For the adsorption experiments, anionic dye AB93 and cationic dye MB were used in this study. The bioadsorbent (20−30 mesh) was added into 200 mL of dye solution for 90 min except for the contact time study. The amount of residual dye in the solution was traced by UV−vis spectra (UV-2900, Hitachi), and the dye concentration was calculated by the absorbance at the maximum absorption.

The effect of initial dye concentration on the adsorption capacity was investigated in a range from 200 to 2500 mg L^{-1} with a bioadsorbent dosage of 0.4 g at 25 °C. The effect of bioadsorbent dosage on the dye removal efficiency was investigated in a range from 0.1 to 0.5 g with a dye initial concentration of 200 mg L^{-1} at 25 °C. The effects of contact time (0 to 150 min), pH (5 to 9), and temperature (20 to 70 °C) were also investigated with 0.4 g of bioadsorbent and dye initial concentration of 200 mg L^{-1}, respectively. NaCl (0 to 0.6 mol L^{-1}) and SDS (0 to 10 mmol L^{-1}) were used to evaluate the influences of electrolyte and surfactant on the dye removal efficiency. All of the tests were carried out in triplicate. The dye removal was determined according to the following eq 2.

$$\text{dye removal (\%)} = \frac{C_0 - C_t}{C_0} \times 100 \tag{2}$$

Scheme 1. Schematic Drawing for the Synthesis of Cellulose-based Bioadsorbents
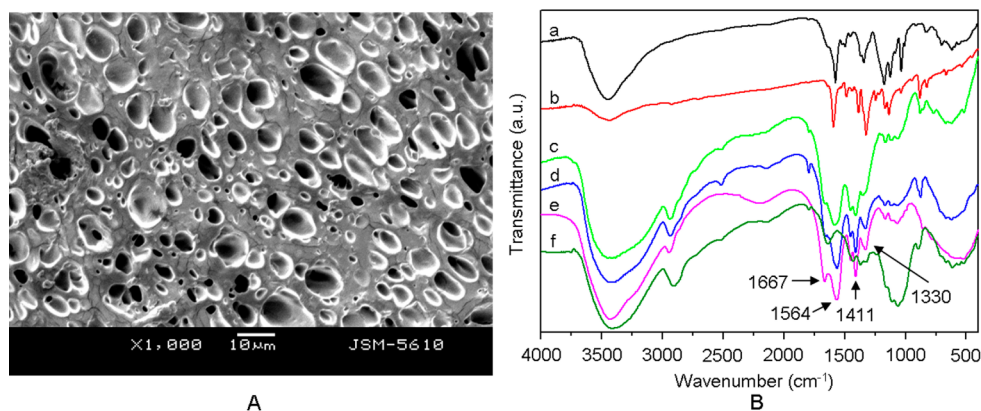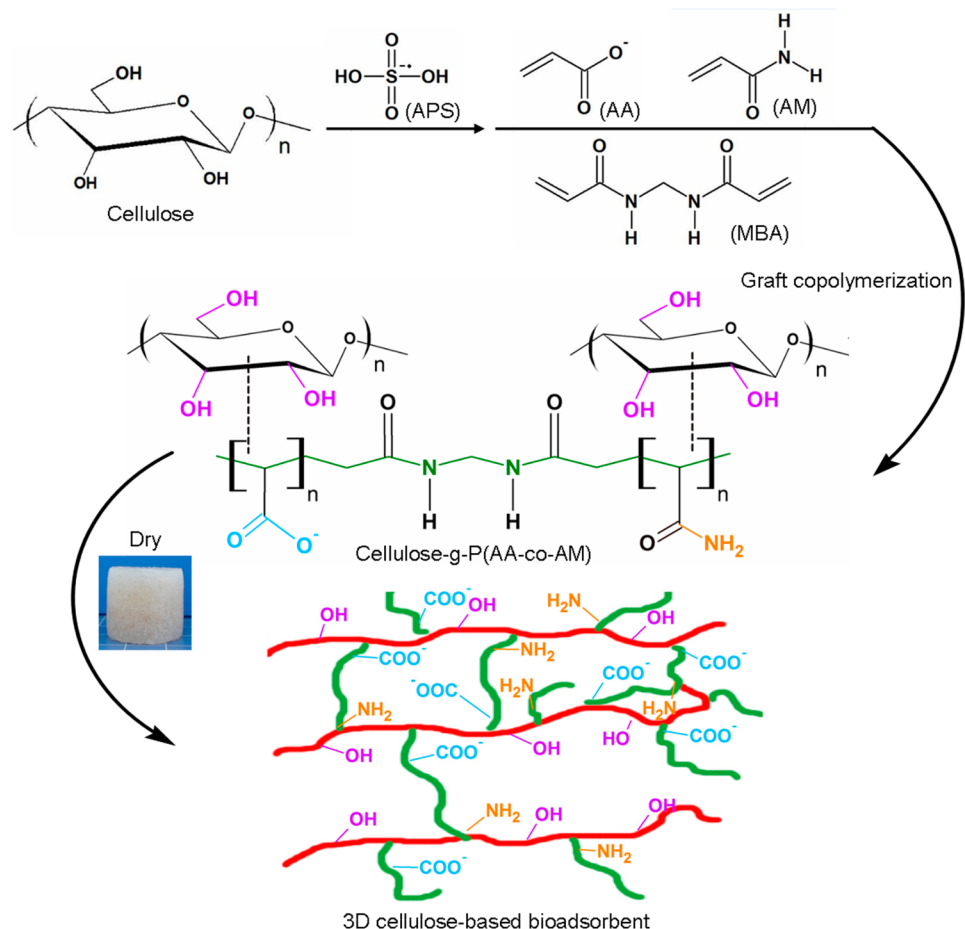

Figure 1. (A) SEM image, and (B) FTIR spectra of (a) AB93, (b) MB, (c) AB93 loaded cellulose-based bioadsorbent, (d) MB loaded cellulose-based bioadsorbent, (e) cellulose-based bioadsorbent, and (f) cellulose.

where C_0 and C_t are the initial and t time concentrations of dye in solution (mg L^{-1}), respectively.

Adsorption of Dyes in Binary Systems. To investigate the dye removal efficiency in more complex systems, AB93 and MB were added into aqueous solution (200 mL) with various mass ratios at a certain concentration of 200 mg L^{-1}. NaCl and SDS were simultaneously added to the binary-dye solutions to evaluate the adsorption capacity of the bioadsorbent at a certain dosage of 0.4 g at 25 °C. For binary system, components A (AB93) and B (MB) were tested at λ_1 and λ_2 to determine the optical densities of d_1 and d_2, respectively. Dye concentrations were calculated using eqs 3 and 4.[45−47]

$$C_A = (k_{B2}d_1 - k_{B1}d_2)/(k_{A1}k_{B2} - k_{A2}k_{B1}) \qquad (3)$$

$$C_B = (k_{A1}d_2 - k_{A2}d_1)/(k_{A1}k_{B2} - k_{A2}k_{B1}) \qquad (4)$$

where k_{A1}, k_{B1}, k_{A2}, and k_{B2} are the calibration constants for components A and B at wavelengths of λ_1 and λ_2, respectively.

Recyclability. The recyclability of the bioadsorbent was measured at 25 °C. 0.4 g of bioadsorbents was added into 200 mL of 200 mg L^{-1} dye solutions for 90 min, then taken out from the solutions. The desorption and regeneration of the bioadsorbents adsorbed by dyes were performed by placing these bioadsorbents into 30 mL of 0.1 mol L^{-1} NaOH solution under agitating at 25 °C for 60 min. The

regenerated adsorbents were used for another adsorption in the subsequent cycles.

RESULTS AND DISCUSSION

Synthesis and Characterization of Bioadsorbent. The cellulose-g-poly(acrylic acid-co-acrylamide) bioadsorbents were synthesized by free-radical graft copolymerization. The whole strategy is presented in Scheme 1. The functional groups such as $-COO^-$ and $-CO-NH_2$ were grafted in the cellulose skeleton from acrylic acid and acrylamide. The interconnected three-dimensional porous structure in the polymer matrix was formed by cross-linking reaction with a pore size of ca. 5−10 μm (Figure 1A).[43,44] These structure changes in cellulose-based bioadsorbent would provide more adsorption sites for adsorbates, and high surface area (363.6 m^2 g^{-1} from BET), which would allow adsorption on both the exterior and interior of the bioadsorbents, consequently possessing high adsorption efficiency.

The FTIR spectra of cellulose and the cellulose-based bioadsorbent are shown in Figure 1B. In the spectrum of raw cellulose (Figure 1f), the characteristic peaks at 3426, 2910, 1438, 1376, 1122, 1066, and 895 cm^{-1} were the typical bands of cellulose molecules.[35,37,48] The peak at 1639 cm^{-1} was assigned to the adsorbed water.[40] Compared with the spectrum of cellulose, new peaks at 1667, 1564, 1411, and 1330 cm^{-1} in the spectrum of bioadsorbent were found (Figure 1e). The peaks at 1667 and 1564 cm^{-1} were attributed to the stretching vibration of CO−NH, and the asymmetric stretching vibration of COOH, respectively.[49,50] The peaks at 1411 and 1330 cm^{-1} were assigned to the symmetrical stretching vibration of COOH, and C−OH in-plane bending, respectively.[37] Moreover, the peak at 3434 cm^{-1} became sharper and stronger, assigning to N−H stretching vibration, which overlapped with O−H groups. These results confirmed that the acrylic acid and acrylamide monomers were successfully grafted onto the cellulose molecules, providing more adsorption sites for dye adsorption.[37,49] Based on the chemical titration methods,[35,36] the contents of carboxyl group and amino group on the bioadsorbent were 10.3 and 8.6 mmol g^{-1}, respectively.

Water Absorbency. The water uptake as a function of time was performed at various pH values at 25 °C. The pH value of the aqueous solution was adjusted using hydrochloric acid (0.05 mol L^{-1}) or sodium hydroxide (0.05 mol L^{-1}). As shown in Figure 2, the pH val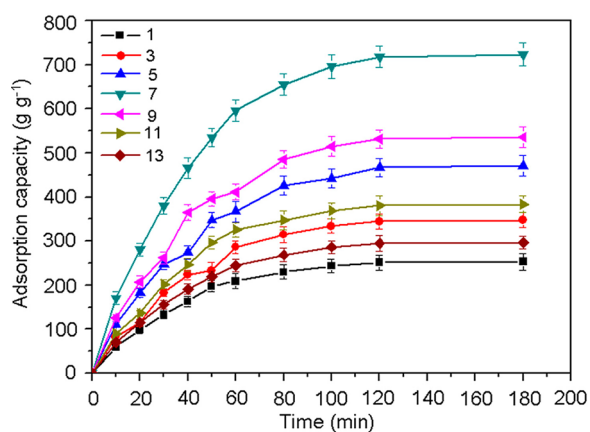ue of the solution significantly affected the adsorption behavior, because the water adsorption capacity of the bioadsorbent increased with the increase of pH values from 1 to 7, then decreased from 9 to 13. It could be observed that pH 7 was the optimum value for the adsorption process with a maximum adsorption capacity of 723.6 g g^{-1}. Nonetheless, the superabsorbent property of bioadsorbent was obtained from pH 5 to pH 11. Regardless of pH value, all the bioadsorbents reached a swelling equilibrium after immersed in water for 120 min. These results could be explained by the facts of protonation and deprotonation of −COOH and −NH$_2$ functional groups at various pH conditions. At strongly acidic conditions (pH < 5), most −COOH and -NH$_2$ groups are protonated into −COOH and −NH$_3^+$ groups.[35,49] The charge shielding effect of Cl$^-$ counterions in medium shields the repulsion of −NH$_3^+$ groups, resulting in the lower water absorbency. Similarly, although most −COO$^-$ groups appear at the extreme alkaline conditions (pH > 11), the decreased adsorption capacity can be observed due to the charge shielding effect of Na$^+$.[43] However, at pH 5−11, large amounts of −COO$^-$ and −NH$_3^+$ groups are contributed to higher water absorbency.

Adsorption of Dyes in Single System. The adsorption behaviors of cellulose-based bioadsorbents to AB93 and MB were investigated in single systems. The effects of initial dye concentration, bioadsorbent dosage, contact time, solution pH, temperature, ionic strength, and surfactant content on dye removal efficiency were investigated comprehensively.

Effect of Initial Dye Concentration and Adsorption Isotherm. The effects of initial concentration of AB93 and MB on dye adsorption capacity were investigated in a range from 200 to 2500 mg L^{-1} at pH 7.0 for 90 min. The dye adsorption capacities onto bioadsorbent increased with the increase of the concentration of dye solutions (Figure 3a). The maximum adsorption capacities for both AB93 and MB reached to 1372 mg g^{-1} at the initial concentration of 2500 mg L^{-1}, which were higher than those of other cellulose-based adsorbents.[35−37] The removal efficiencies for AB93 and MB initially increased and then decreased (Figure 3b), which might be due to the fact that large numbers of vacant active sites were available for the adsorption at a lower initial concentration, and then saturated sites were difficult to capture the dye molecules.[49] In the case of MB, the removal efficiency was higher than AB93 at the low initial concentration, which probably was due to the smaller spatial prohibition in the molecular structure of MB and its positive feature making it more accessible to the adsorption sites of cellulose-based bioadsoebent.[37,49] However, the decrease in the removal efficiency of MB was more obvious than that of AB93 when the initial concentration was more than 800 mg L^{-1}. This result could be explained by the presence of three sulfo and three amine groups in the structure of AB93 dye molecule, which made more affinity for the adsorption of AB93 than that for MB at higher concentrations.[46,47]

Equilibrium adsorption isotherms, namely Langmuir and Freundlich, were applied to analyze the adsorption data of AB93 and MB on the bioadsorbents, and their linear equations are presented below.[51,52]

$$\frac{C_e}{q_e} = \frac{1}{b q_{max}} + \frac{C_e}{q_{max}} \tag{5}$$

$$\ln q_e = \ln K_f + \frac{\ln C_e}{n} \tag{6}$$

Figure 2. Water absorbency of cellulose-based bioadsorbents at different solution pH values.
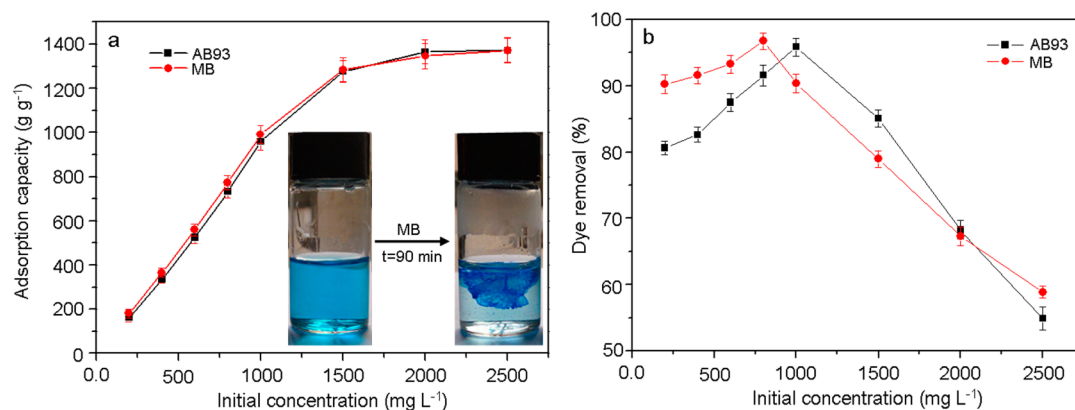
Figure 3. Effect of initial dye concentration on (a) adsorption capacity, and (b) dye removal efficiency of AB93 and MB using the cellulose-based bioadsorbents.

Table 2. Isotherm Parameters for the Adsorption of AB93 and MB onto Cellulose-based Bioadsorbent

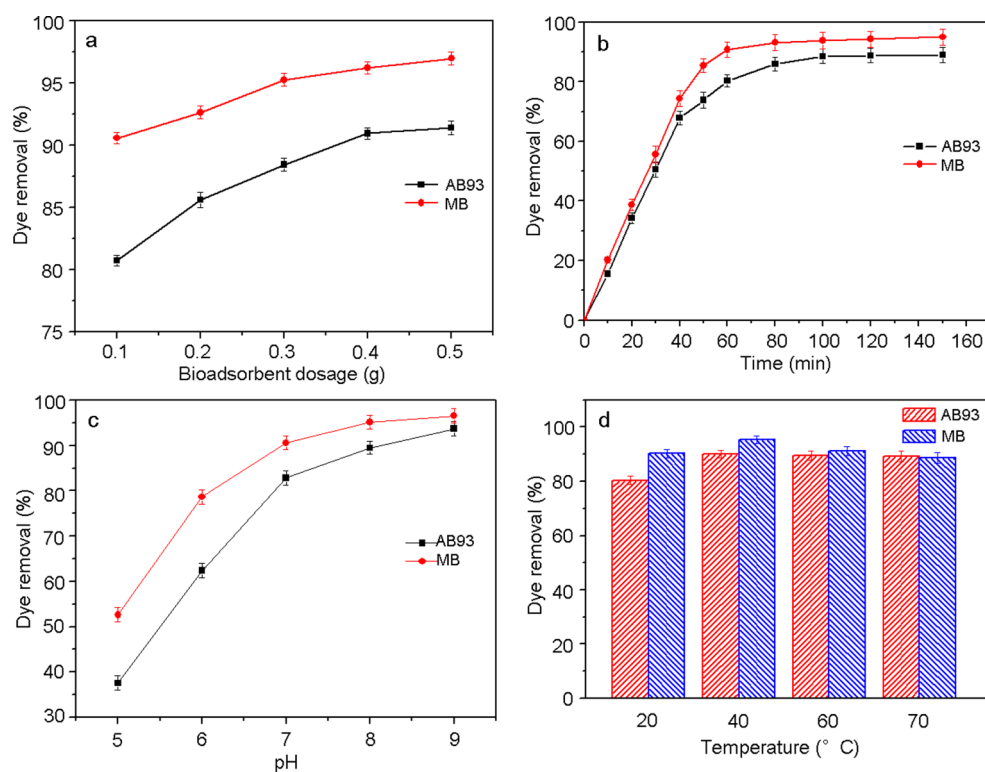|	Langmuir isotherm			Freundlich isotherm		
	b (L mg^{-1})	q_{max} (mg g^{-1})	R^2	K_f (L mg^{-1})	n	R^2
AB93	5.12×10^{-3}	1602	0.9373	13.17	1.30	0.9730
MB	5.91×10^{-2}	1814	0.9663	15.66	1.37	0.9736

Figure 4. Effects of (a) bioadsorbent dosage, (b) contact time, (c) solution pH, and (d) temperature on the dye removal efficiencies of AB93 and MB using the cellulose-based bioadsorbents.

where q_e and q_{max} (mg g^{-1}) are the adsorption capacity at equilibrium and the maximum adsorption capacity according to Langmuir monolayer adsorption. C_e (mg L^{-1}) is the equilibrium concentration of dye. b (L mg^{-1}) is the Langmuir constant, relates to free energy and affinity of the adsorbate for the binding sites. K_f (L mg^{-1}) and n are Freundlich constants related to adsorption capacity and adsorption intensity of the bioadsorbent, respectively.

The relative parameter values calculated from the Langmuir and the Freundlich models are listed in Table 2. For Langmuir model, q_{max}, which is a measure of monolayer adsorption capacity of the bioadsorbents, was calculated as 1602 mg g^{-1} for AB93 and 1814 mg g^{-1} for MB. The values of b were found to be within the range from 0 to 1, indicating that the cellulose-based bioadsorbents were suitable for adsorption of AB93 and MB. For Freundlich model, the values of K_f showed that adsorption of AB93 and MB on the bioadsorbents was easy and

Table 3. Kinetic Parameters of Pseudo-First-Order and Pseudo-Second-Order models for the Adsorption of AB93 and MB onto Cellulose-based Bioadsorbent

	pseudo-first-order model			pseudo-second-order model		
	k_1 (min^{-1})	q_e (mg g^{-1})	R^2	k_2 (g mg^{-1} min^{-1})	q_e (mg g^{-1})	R^2
AB93	0.039	73.28	0.9905	1.67×10^{-5}	104.49	0.9981
MB	0.036	79.19	0.9931	1.30×10^{-5}	108.11	0.9988

adsorption capacities increased with the increases of initial concentrations. The value of n reveals the favorability and capacity of the adsorption system. Calculated from Freundlich model, $n > 1$ confirmed favorable adsorption conditions. By comparing the results obtained from the two isotherm models, due to higher R^2 values, the Freundlich model was the better fit, indicating that the adsorption of AB93 and MB on the cellulose-based bioadsorbents was a heterogeneous surface with multilayer sorption.[51,52] Similar observation was reported for the removal of methylene blue and methyl violet using a nanocomposite of hydrolyzed polyacrylamide grafted xanthan gum and incorporated nanosilica.[51]

Effect of Bioadsoebent Dosage. Figure 4a shows the effect of bioadsorbent dosage on the dye removal efficiency by contacting 200 mL of dye solution with an initial concentration of 200 mg L^{-1} at 25 °C for 90 min. The dye removal efficiency increased dramatically with increasing the bioadsorbent dosage, which was due to the increase of available adsorption sites in cellulose-based bioadsorbents. The optimum bioadsorbent dosages for both AB93 and MB were selected as 0.4 g for 200 mL of 200 mg L^{-1} dye solution. The removal efficiencies for AB93 and MB reached up to 91.0% and 96.2%, respectively.

Effect of Contact Time and Adsorption kinetics. By changing the contact time from 0 to 150 min, the dye could be removed rapidly in the first 40 min (Figure 4b). The adsorption equilibrium reached at about 80 min. To obtain better adsorption efficiency, 100 min was chosen here for the investigation of two dyes, in which 93.8% of MB and 88.6% of AB93 were removed, respectively. In the adsorption process, the dye molecules migrated from aqueous solution onto the surface of the bioadsorbent, and then were adsorbed through the van der Waals force. Subsequently, the electrostatic interactions occurred when the anionic dye AB93 or cationic dye MB were close enough to the adsorption sites ($-COO^-$, $-NH_2$) on the surface of cellulose-based bioadsorbent.[35,37] The accumulation of dye molecules on the adsorption sites of the bioadsorbent increased with the contact time, but appearing a plateau which might be resulted from the strong repulsive forces between the dye molecules on the adsorbent.[37]

To further investigate the adsorption mechanism and its potential rate-controlling steps such as mass transfer, diffusion control and chemical reaction, pseudo-first-order kinetic model and pseudo-first-order kinetic model were employed.[51,52] The constants of both kinetic models were calculated using eqs 7 and 8.

$$\ln(q_e - q_t) = \ln q_e - k_1 t \tag{7}$$

$$\frac{t}{q_t} = \frac{t}{q_e} + \frac{1}{k_2 q_e^2} \tag{8}$$

where q_e and q_t (mg g^{-1}) are the adsorption capacities at equilibrium and at time t, respectively. k_1 (min^{-1}) and k_2 (g mg^{-1} min^{-1}) are the rate constants of pseudo-first-order and pseudo-second-order, respectively.

As can be seen in Table 3, the values of R^2 for AB93 and MB obtained from the pseudo-second-order kinetic model were found to be over 0.998, making them higher than those of the pseudo-first-order kinetic model. The results indicated that the adsorption of AB93 and MB onto the bioadsorbents was well described by the pseudo-second-order kinetic model. And the rate-controlling step in adsorption of dyes was chemisorption including valence forces through sharing or exchanging of electrons between adsorbent and adsorbate.[6,51]

Effect of pH Value. Based on the results of water absorbency at different pH values as described above, the adsorption of dyes on the bioadsorbent was investigated by changing the solution pH value from 5 to 9 (Figure 4c). It was found that the adsorptions of AB93 and MB on bioadsorbent increased rapidly at pH 5−7, and then slowed at pH 7−9. The maximum removal efficiencies of AB93 and MB at pH 9 were 93.7% and 96.5%, respectively.

It is known that the solution pH is an important parameter during the dye adsorption process, and it can affect the surface charge of the adsorbent, the degree of ionization of dyes as well as the structure of the dye molecules. The results of blank dye solutions showed that changing the pH value of the dye solution had a negligible effect on the maximum absorption wavelength of AB93 and MB dyes (data no shown), suggesting that there was no chemical structure change of dye molecule. In the acidic solution, the bioadsorbent is protonated, and the excessive H$^+$ ions on the surface of bioadsorbent compete with the dye molecules, resulting in the low dye adsorption. In the alkaline solution, the bioadsorbent is deprotonated, and the electrostatic interaction between bioadsorbent and dye molecules increases resulting in a higher dye adsorption.[35,37,49]

The propensity can be assessed through the ζ-potential at different pH values. As can be seen from Figure S1 (Supporting Information), all the bioadsorbent ζ-potentials were negative, but increased from −16.13 to −65.90 mV as the pH value increases from 5 to 9. The bioadsorbent surface became more negatively charged, thereby strengthening the repulsive interactions between the bioadsorbents and providing more adsorption sites. The adsorption mechanism was discussed in detail in the Adsorption Mechanism section.

Effect of Temperature. Generally, the dye removal efficiencies increased with the increase of temperature, and then kept constant (Figure 4d). For AB93, the removal efficiency increased from 80.4% to 90.2% with the increase of temperature from 20 to 40 °C, and then kept constant. By comparison, a maximum adsorption of 95.4% was observed for MB at 40 °C. It is well-known that the increase of temperature may enhance the mobility of dye molecules, and also provide sufficient energy to facilitate the interaction between the dye molecules and the adsorption sites at the surface of bioadsorbent. Furthermore, the increase of temperature may induce a swelling effect with the internal structure of bioadsorbent, which enable the passage of more dye molecules.[46] These facts finally result in the increase of dye adsorption. At a higher temperature (60−70 °C), desorption
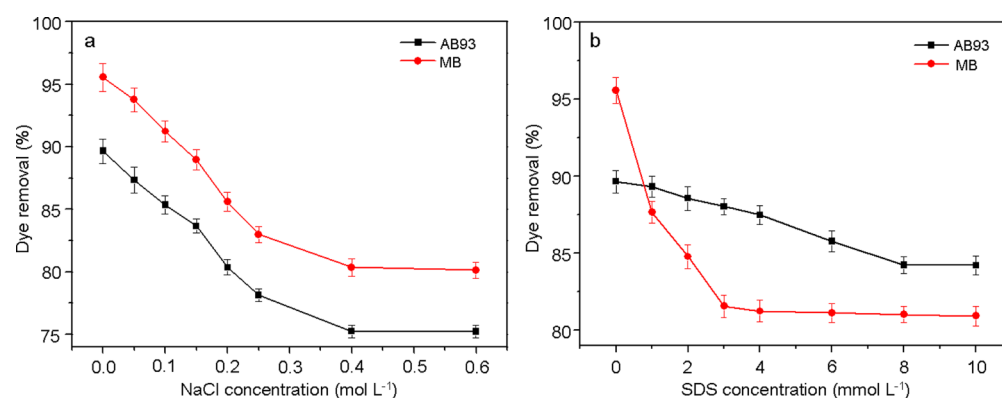
Figure 5. Effects of (a) NaCl and (b) SDS concentrations on the dye removal efficiencies of AB93 and MB using the cellulose-based bioadsorbents.
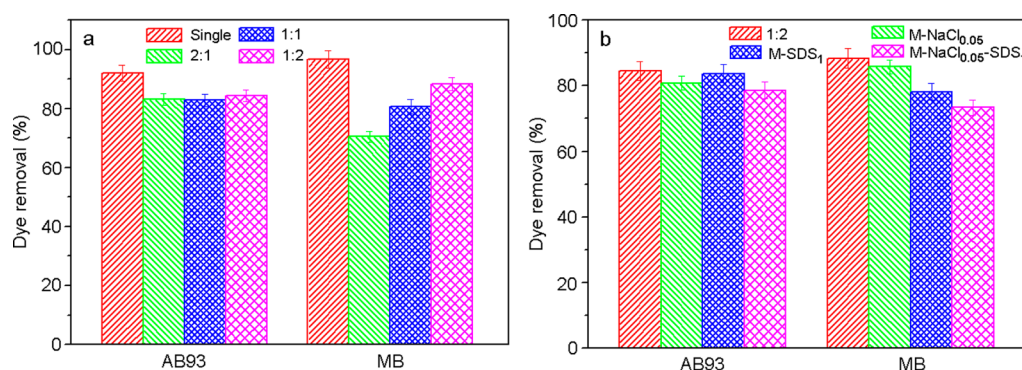

Figure 6. Dye removal efficiencies of AB93 and MB in (a) binary-dye solution and (b) complex solutions. (a) mass ratios of AB93 to MB are 2:1, 1:1, 1:2; (b) contents of NaCl and SDS are 0.05 M and 1 mM at fixed mass ratio of 1:2 for AB93 to MB.

behavior may dominate during adsorption process for the violent molecular motion,[51] consequently reducing the adsorption capacity. Thus, the temperature was kept at 25 °C for other investigations in this work.

Effect of Ionic Strength. Here, NaCl was used to investigate the effect of ionic strength on the removal efficiency of AB93 and MB. As shown in Figure 5a, the removal efficiencies for both AB93 and MB decreased with the increase of NaCl contents from 0 to 0.6 mol L^{-1} in the dye solutions. This result could be explained by a competitive effect between the salt ions (Na$^+$ and Cl$^-$) and the dyes (cationic MB and anionic AB93) with functional surface of the cellulose-based bioadsorbent (−COO$^-$, −NH$_3^+$, and −OH). Similar results were reported for the removal of MB and MV using a nanocomposite of hydrolyzed polyacrylamide grafted xanthan gum and incorporated nanosilica,[51] and for the removal of AB194 using chitosan/zeolite biocomposite bead.[52] With the increase of NaCl contents, the shielding effect of ions for charged dye molecules was enhanced, resulting in the reduce of adsorption efficiencies.[52,53] This result indicated that the adsorption might result from the electrostatic interactions between the adsorbents and the dye molecules.[37,51,52]

Effect of Surfactant. Surfactants (e.g., leveling agent) are widely used for the textile dyeing and dyeing industries. Thus, it is important to investigate the effect of surfactant (SDS) content on the adsorption capacity of bioadsorbent. Figure 5b showed that the removal efficiency of AB93 gradually declined with the increase of SDS contents. However, the removal efficiency of MB dramatically decreased from 96% to 82% when the SDS content was increased to 3 mmol L^{-1}, then kept a certain value with further increase of SDS contents. The

difference between AB93 and MB may be due to the fact that SDS is an anionic surfactant, which can compete with the bioadsorbent to bond MB cationic dye, forming stable SDS-MB aggregates, consequently reducing dye adsorption on the bioadsorbents.[54]

Adsorption of Dyes in Binary Systems. In industrial wastewater, various types of dissolved substances like dyes, salts, surfactants, and metal ions commonly exist, which may compete for the adsorption sites on the surface of adsorbent, and consequently decrease the removal efficiency of dye. To investigate the adsorption capacity of cellulose-based bioadsorbent in the complex water, NaCl and SDS were added into the binary-dye solution. The mass ratio of AB93 and MB in solution was designed to 2:1, 1:1, and 1:2, whereas the contents of NaCl and SDS were designed to 0.05 M and 1 mM, respectively. The samples are defined as M-NaCl$_{0.05}$, M-SDS$_1$, and M-NaCl$_{0.05}$-SDS$_1$ based on the contents of NaCl and SDS in the mixed solutions.

Effect of Mass Ratio. Figure 6a shows the adsorption efficiencies of the bioadsorbent in binary-dye solutions at different mass ratios of AB93 and MB, indicating that the dye adsorption profiles were different in the binary systems. The bioadsorbent exhibited the initial adsorption efficiencies of 92.1% for AB93, and 96.7% for MB, respectively. But when another dye was added, the adsorption decreased. Especially, the adsorption of MB increased as the mass ratio, but the adsorption of AB93 almost did not change.

Dye Adsorption in Binary Systems. Figure 6b shows the effects of dye auxiliaries (NaCl and SDS) on the adsorption in binary-dye solutions at a fixed mass ratio of AB93 to MB at 1:2. Compared with the adsorption in binary-dye solution without
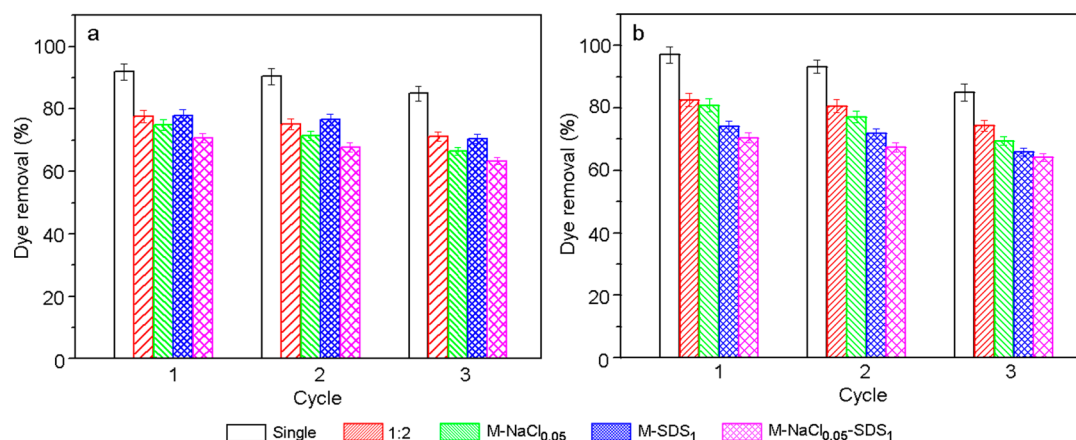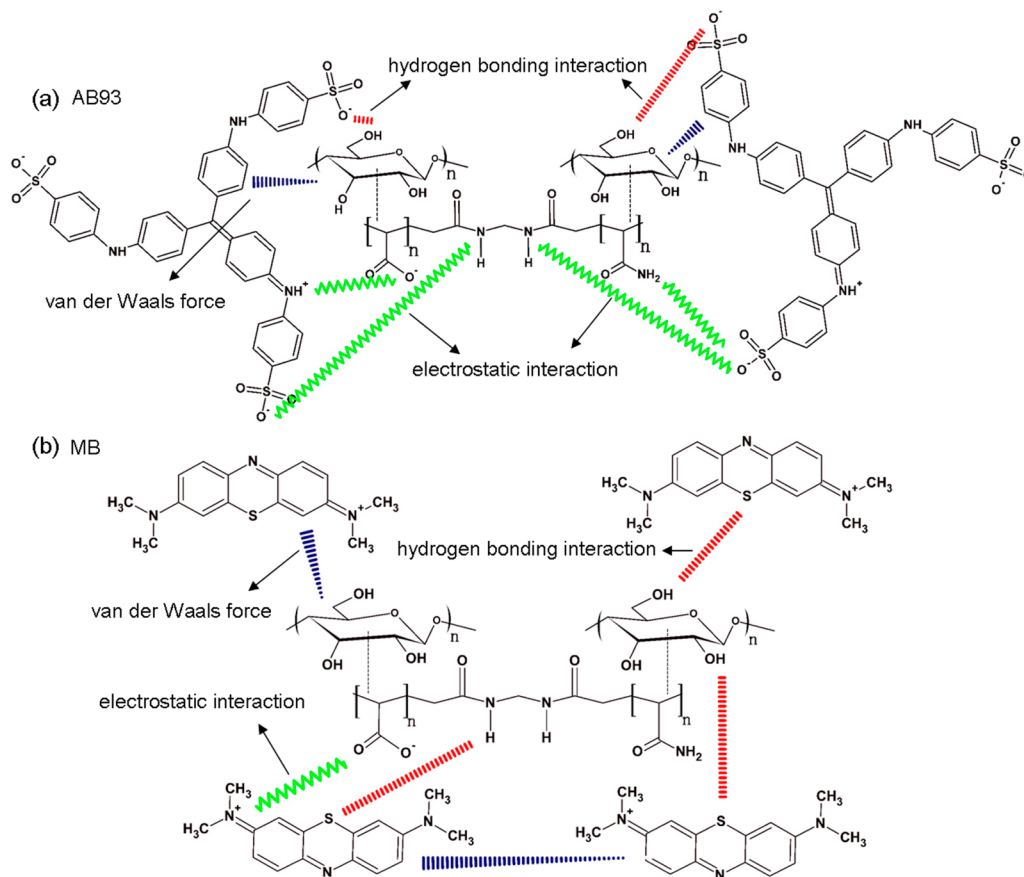
Figure 7. Dye removal efficiencies of (a) AB93 and (b) MB after three desorption/adsorption cycles in complex solutions (contents of NaCl and SDS are 0.05 M and 1 mM at fixed mass ratio of 1:2 for AB93 to MB).

Scheme 2. Schematic Drawing for the Possible Interactions between the Bioadsorbent and (a) AB93 and (b) MB Dye Molecules

dye auxiliaries, the adsorptions of both AB93 and MB were reduced in the complex systems with dye auxiliaries. Nonetheless, the dye removal efficiencies were found to be 78.5% for AB93 and 73.3% for MB, respectively. In addition, the dye auxiliaries presented in the solutions exhibited a stronger effect on the adsorption of MB than that of AB93, probably resulted from the different structures of AB93 and MB. As stated above, AB93 is an anionic dye with three negatively charged sulfonic groups, and MB is a cationic dye with positive surface charge in solution. The dye auxiliary effect here revealed that the adsorption efficiencies decreased with the increase of NaCl and SDS contents, which confirmed that the adsorption of both

dyes on the bioadsorbent was also dominated by the electrostatic interaction in the complex systems. AB93 has higher charge load than MB, which prevents it to be interfered by auxiliaries, ensuring a higher adsorption.[47]

Recyclability. The recyclability of bioadsorbent and the removal efficiency of dyes are important in pollution control and environmental protection. The regeneration of the cellulose-based bioadsorbent was performed by immersing the bioadsorbent into NaOH solution for 60 min. As shown in Figure 7, after three adsorption−harvesting cycles, the recyclable adsorption behavior of bioadsorbent to AB93 and MB was similar and the adsorption capacities of bioadsorbent

decreased slightly. In single systems, the dye removal of bioadsorbent to AB93 after one and three cycles was 92.0% and 85.0%, while that of MB was 97.0% and 85.0%, respectively. For complex systems, although addition of dye auxiliaries had obvious negative effects on the removal of dyes, the adsorption capability of bioadsorbent still remained more than 60% after three cycles. This demonstrated that the cellulose-based bioadsorbent has good recycling ability for the removal of AB93 and MB not only from single solution, but also from complex solutions. The potential of the cellulose-based bioadsorbents in practical application for dye removal will further be studied in continuous flow fixed-bed column in our future study.

Adsorption Mechanism. The adsorption capacity of adsorbent is determined by various factors such as the structure and functional behavior of the adsorbate molecule, surface characteristics of the adsorbent, mass transport process, and so on.[51,55] In this work, both AB93 and MB are planar molecules, and can be easily adsorbed on the cellulose-based bioadsorbents by van der Waals force and hydrogen bonding interactions.[55]

The FTIR spectra of AB93, MB, cellulose-based bioadsorbent, and dye loaded bioadsorbent showed the possible interaction sites between the bioadsorbents and dye molecules (Figure 1B). Compared with the spectra of cellulose-based bioadsorbent, the characteristics peaks for the dye loaded bioadsorbent broadened and shifted slightly (Figure 1c,d). For example, the OH/NH stretching vibration obviously broadened and shifted from 3434 to 3429 cm^{-1} (for AB93) and to 3424 cm^{-1} (for MB), CO$-$NH stretching vibration from 1667 to 1672 cm^{-1} (for AB93) and to 1655 cm^{-1} (for MB), COO$^-$ asymmetric stretching vibration from 1564 to 1582 cm^{-1} (for AB93) and to 1559 cm^{-1} (for MB), COO$^-$ symmetric stretching vibration from 1411 to 1402 cm^{-1} (for AB93) and to 1402 cm^{-1} (for MB), and for C$-$OH in-plane bending, the shift occurred from 1330 to 1347 cm^{-1} (for AB93) and to 1325 cm^{-1} (for MB). However, there was no significant change occurred for peak corresponding to CH stretching vibration at 2942 cm^{-1}. These indicated the specific electrostatic and hydrogen bonding interactions between the functional groups of dye molecules and the bioadsorbents.

Field emission (FE)SEM images were also used to compare the morphological features and surface characteristics of dye loaded bioadsorbents (Figure S2, Supporting Information). Compared with the porous microstructure of the bioadsorbent, the appearance of layers was evidenced from FESEM images for dyes, which resulted from the accumulation of AB93 and MB on the surface of the bioadsorbent. Especially, the effect studies of salt and surfactant confirmed that the electrostatic interactions between dyes and the adsorption sites of the bioadsorbent were the main interaction forces. Moreover, the adsorption capacity and rate commonly depend on the number of available active sites and microstructure of the bioadsorbent.[37,55] Thus, it is presumed that the possible interactions involved in AB93 and MB adsorption process are electrostatic interaction as well as hydrogen bonding interaction. These possible interactions between the dye molecules and the cellulose-based bioadsorbent were then shown in Scheme 2.

CONCLUSIONS

The cellulose-based bioadsorbents were designed and synthesized by graft copolymerization to remove the organic dyes from single and binary systems. The modification of cellulose with acrylic acid and acrylamide was found to effectively increase its adsorption sites, resulting in excellent dye removal efficiency from aqueous solution. The detailed investigation of adsorption behavior of the bioadsorbent revealed that the adsorption process was dominated by the electrostatic interactions between the bioadsorbent and the dye molecules. The results of this study indicated that the cellulose-based bioadsorbent could be successfully used for the removal of dyes from complex aqueous solutions. In addition, the mulberry branches are the byproduct of the sericulture industry, and are actually the waste materials. The utilization of mulberry branches as the raw materials for the adsorbent preparation not only resolves the environment issues but also offers a way to prepare a promising low cost adsorbent for dye removal from industrial wastewater.

ASSOCIATED CONTENT

Ⓢ Supporting Information

ζ-potential values of cellulose-based bioadsorbent at different pH. FESEM images of cellulose-based bioadsorbent after dye adsorption. This material is available free of charge via the Internet at http://pubs.acs.org.

AUTHOR INFORMATION

Corresponding Author

*Professor Ju Ming Yao. E-mail: yaoj@zstu.edu.cn. Tel: +86-571-86843618. Fax: +86-571-86843619.

Notes

The authors declare no competing financial interest.

ACKNOWLEDGMENTS

REFERENCES

(1) Xie, Y. J.; Yan, B.; Xu, H. L.; Chen, J.; Liu, Q. X.; Deng, Y. H.; Zeng, H. B. Highly regenerable mussel-inspired Fe_3O_4@polydopamin-Ag core-shell microspheres as catalyst and adsorbent for methylene blue removal. *ACS Appl. Mater. Interfaces* **2014**, *6*, 8845−8852.

(2) Yan, H.; Li, H. J.; Tao, X.; Li, K.; Yang, H.; Li, A. M.; Xiao, S. J.; Cheng, R. S. Rapid removal and separation of iron(II) and manganese(II) from micropolluted water using magnetic graphene oxide. *ACS Appl. Mater. Interfaces* **2014**, *6*, 9871−9880.

(3) Unuabonah, E. I.; Gunter, C.; Weber, J.; Lubahn, S.; Taubert, A. Hybrid clay: A new highly efficient adsorbent for water treatment. *ACS Sustainable Chem. Eng.* **2013**, *1*, 966−973.

(4) Amaral, F. M.; Kato, M. T.; Florencio, L.; Gavazza, S. Color, matter and sulfate removal from textile effluents by anaerobic and aerobic processes. *Bioresour. Technol.* **2014**, *163*, 364−369.

(5) Zhao, S. P.; Zhou, F.; Li, L. Y.; Cao, M. J.; Zuo, D. Y.; Liu, H. T. Removal of anionic dyes from aqueous solutions by adsorption of chitosan-based semi-IPN hydrogel composites. *Composites, Part B* **2012**, *43*, 1570−1578.

(6) Zhang, S. X.; Zhang, Y. Y.; Bi, G. M.; Liu, J. S.; Wang, Z. G.; Xu, Q.; Xu, H.; Li, X. Y. Mussel-inspired polydopamine biopolymer decorated with magnetic nanoparticles for multiple pollutants removal. *J. Hazard. Mater.* **2014**, *270*, 27−34.

(7) Mathieu-Denoncourt, J.; Martyniuk, C. J.; de Solla, S. R.; Balakrishnan, V. K.; Lanqlois, V. S. Sediment contaminated with the azo dye disperse yellow 7 alters cellular stress- and androgen-related transcription in silurana tropicalis larvae. *Environ. Sci. Technol.* **2014**, *48*, 2952−2961.

(8) de Luna, L. A.; da Silva, T. H.; Nogueira, R. F.; Kummrow, F.; Umbuzeiro, G. A. Aquatic toxicity of dyes before and after photo-Fenton treatment. *J. Hazard. Mater.* **2014**, *276*, 332−338.

(9) An, J. S.; Back, Y. J.; Kim, K. C.; Cha, R.; Jeong, T. Y.; Chung, H. K. Optimization for the removal of orthophosphate from aqueous solution by chemical precipitation using ferrous chloride. *Environ. Technol.* **2014**, *35*, 1668−1675.

(10) Li, C. R.; Zhuang, Z. Y.; Huang, F.; Wu, Z. C.; Hong, Y. P.; Lin, Z. Recycling rare earth elements from industrial wastewater with flowerlike nano-Mg(OH)$_2$. *ACS Appl. Mater. Interfaces* **2013**, *5*, 9719−9725.

(11) Du, X.; Zhang, H.; Hao, X.; Guan, G.; Abudula, A. Facile preparation of ion-imprinted composite film for selective electrochemical removal of nickel(II) ions. *ACS Appl. Mater. Interfaces* **2014**, *6*, 9543−9549.

(12) Fu, L.; Shuang, C.; Liu, F.; Li, A.; Li, Y.; Zhou, Y.; Song, H. Rapid removal of copper with magnetic poly-acrylic weak acid resin: Quantitative role of bead radius on ion exchange. *J. Hazard. Mater.* **2014**, *272*, 102−111.

(13) Wei, X. Z.; Kong, X.; Wang, S. X.; Xiang, H.; Wang, J. D.; Chen, J. Y. Removal of heavy metals from electroplating wastewater by thin-film composite nanofiltration hollow-fiber membranes. *Ind. Eng. Chem. Res.* **2013**, *52*, 17583−17590.

(14) Liu, W.; Wu, Z. L.; Wang, Y. J.; Zhao, Y. L.; Liu, W. C.; Yu, Y. Recovery of isoflavones from the soy whey wasterwater using two-stage batch foam fractionation. *Ind. Eng. Chem. Res.* **2013**, *52*, 13761−13767.

(15) Deng, S. J.; Wang, R.; Xu, H. J.; Jiang, X. S.; Yin, J. Hybrid hydrogels of hyperbranched poly(ether amine)s (hPEAs) for selective adsorption of guest molecules and separation of dyes. *J. Mater. Chem.* **2012**, *22*, 10055−10061.

(16) Deng, S. J.; Xu, H. J.; Jiang, X. S.; Yin, J. Poly(vinyl alcohol) (PVA)-enhanced hybrid hydrogels of hyperbranched poly(ether amine)s (hPEAs) for selective adsorption and separation of dyes. *Macromolecules* **2013**, *46*, 2399−2406.

(17) Li, B.; Dong, Y. C.; Zou, C.; Xu, Y. M. Iron (III)-alginate fiber complex as a highly effective and stable heterogeneous Fenton photocatalyst for mineralization of organic dye. *Ind. Eng. Chem. Res.* **2014**, *53*, 4199−4206.

(18) Yadav, A.; Mukherji, S.; Garg, A. Removal of chemical oxygen demand and color from simulated textile wastewater using a combination of chemical/physicochemical processes. *Ind. Eng. Chem. Res.* **2013**, *52*, 10063−10071.

(19) Rodrigues, C. S. D.; Madeira, L. M.; Boaventura, R. A. Decontamination of an industrial cotton dyeing wastewater by chemical and biological processes. *Ind. Eng. Chem. Res.* **2014**, *53*, 2412−2421.

(20) Tastan, B. E.; Karatay, S. E.; Donmez, G. Bioremoval of textile dyes with different chemical structures by *Aspergillus versicolor* in molasses medium. *Water Sci. Technol.* **2012**, *66*, 2177−2184.

(21) Liu, F.; Chung, S.; Oh, G.; Seo, T. S. Three-dimensional graphene oxide nanostructure for fast and efficient water-soluble dye removal. *ACS Appl. Mater. Interfaces* **2012**, *4*, 922−927.

(22) Dou, X. Q.; Li, P.; Zhang, D.; Feng, C. L. C$_2$-symmetric benzene-based hydrogels with unique layered structures for controllable organic dye adsorption. *Soft Matter* **2012**, *8*, 3231−3238.

(23) Zhu, X. D.; Liu, Y. C.; Zhou, C.; Zhang, S. C.; Chen, J. M. Novel and high-performance magnetic carbon composite prepared from waste hydrochar for dye removal. *ACS Sustainable Chem. Eng.* **2014**, *2*, 969−977.

(24) Cifuentes, A. R.; Avila, K.; García, J. C.; Daza, C. E. The pyrolysis of rose stems to obtain activated carbons: A study on the adsorption of Ni(II). *Ind. Eng. Chem. Res.* **2013**, *52*, 16197−16205.

(25) Zhang, C. M.; Song, W.; Sun, G. H.; Xie, L. J.; Wan, L.; Wang, J. L.; Li, K. X. Synthesis, characterization, and evaluation of activated carbon spheres for dibenzothiophene from model diesel fuel. *Ind. Eng. Chem. Res.* **2014**, *53*, 4271−4276.

(26) Liu, L. H.; Lin, Y.; Liu, Y. Y.; Zhu, H.; He, Q. Removal of methylene blue from aqueous solutions by sewage sludge based granular activated carbon: Adsorption equilibrium, kinetics, and thermodynamics. *J. Chem. Eng. Data* **2013**, *58*, 2248−2253.

(27) Magnacca, G.; Allera, A.; Montoneri, E.; Celi, L.; Benito, D. E.; Gagliardi, L. G.; Gonzalez, M. C.; Martire, D. O.; Carlos, L. Novel magnetite nanoparticles coated with waste-sourced biobased substances as sustainable and renewable adsorbing materials. *ACS Sustainable Chem. Eng.* **2014**, *2*, 1518−1524.

(28) Nayab, S.; Farrukh, A.; Oluz, Z.; Tuncel, E.; Rashid, S. Design and fabrication of branched polyamine functionalized mesoporous silica: An efficient absorbent for water remediation. *ACS Appl. Mater. Interfaces* **2014**, *6*, 4408−4417.

(29) Zhou, Y. B.; Gu, X. C.; Zhang, R. Z.; Lu, J. Removal of aniline from aqueous solution using pine sawdust modified with citric acid and *β*-cyclodextrin. *Ind. Eng. Chem. Res.* **2014**, *53*, 887−894.

(30) Zhang, X.; Li, G. H.; Zhang, H. Q.; Wang, X. M.; Qu, J. Y.; Liu, P. G.; Wang, Y. N. Enhanced adsorption capacity and selectivity toward salicylic acid in water by a cationic polymer functionalized 3-D ordered macroporous adsorbent. *Soft Matter* **2013**, *9*, 6159−6166.

(31) Kuwahara, Y.; Tamagawa, S.; Fujitani, T.; Yanashita, H. A novel conversion process for waste slag: Synthesis of calcium silicate hydrate from blast furnace slag and its application as a versatile adsorbent for water purification. *J. Mater. Chem. A* **2013**, *1*, 7199−7210.

(32) Yu, X. L.; Tong, S. R.; Ge, M. F.; Zuo, J. C.; Cao, C. Y.; Song, W. G. One-step synthesis of magnetic composites of cellulose@iron oxide nanoparticles for arsenic removal. *J. Mater. Chem. A* **2013**, *1*, 959−965.

(33) Tu, K.; Wang, Q. Y.; Lu, A.; Zhang, L. N. Portable visible-light photocatalysts constructed from Cu$_2$O nanoparticles and graphene oxide in cellulose matrix. *J. Phys. Chem. C* **2014**, *118*, 7202−7210.

(34) Iwamoto, S.; Isogai, A.; Iwata, T. Structure and mechanical properties of wet-spun fibers made from natural cellulose nanofibers. *Biomacromolecules* **2011**, *12*, 831−836.

(35) Zhou, Y. M.; Zhang, M.; Hu, X. Y.; Wang, X. H.; Niu, J. Y.; Ma, T. S. Adsorption of cationic dyes on a cellulose-based multicarboxyl adsorbent. *J. Chem. Eng. Data* **2013**, *58*, 413−421.

(36) Bayramoglu, G.; Altintas, B.; Arica, M. Y. Synthesis and characterization of magnetic beads containing aminated fibrous surfaces for removal of reactive green 19 dye: Kinetics and thermodynamic parameters. *J. Chem. Technol. Biotechnol.* **2012**, *87*, 705−713.

(37) Zhou, Y. M.; Zhang, M.; Wang, X. H.; Huang, Q.; Min, Y. H.; Ma, T. S.; Niu, J. Y. Removal of crystal violet by a novel cellulose-based adsorbent: Comparison with native cellulose. *Ind. Eng. Chem. Res.* **2014**, *53*, 5498−5506.

(38) Bonenfant, D.; Niquette, P.; Mimeault, M.; Hausler, R. Adsorption and recovery of nonylphenol ethoxylate on a crosslinked beta-cyclodextrin-carboxymethylcellulose polymer. *Water Sci. Technol.* **2010**, *61*, 2293−2301.

(39) Chen, L.; Berry, R. M.; Tam, K. C. Synthesis of *β*-cyclodextrin-modified cellulose nanocrystals (CNCs)@Fe$_3$O$_4$@SiO$_2$ superparamagnetic nanorods. *ACS Sustainable Chem. Eng.* **2014**, *2*, 951−958.

(40) Pei, A. H.; Butchosa, N.; Berglund, L. A.; Zhou, Q. Surface quaternized cellulose nanofibrils with high water absorbency and adsorption capacity of anionic dyes. *Soft Matter* **2013**, *9*, 2047−2055.

(41) Zhou, Y. M.; Zhang, L. L.; Fu, S. Y.; Zheng, L. M.; Zhan, H. Y. Adsorption behavior of Cd^{2+}, Pb^{2+}, and Ni^{2+} from aqueous solutions on cellulose-based hydrogels. *BioResources* **2012**, *7*, 2752−2765.

(42) Li, R. J.; Fei, J. M.; Cai, Y. R.; Li, Y. F.; Feng, J. Q.; Yao, J. M. Cellulose whiskers extracted from mulberry: A novel biomass production. *Carbohydr. Polym.* **2009**, *76*, 94−99.

(43) Wu, F.; Zhang, Y.; Liu, L.; Yao, J. M. Synthesis and characterization of a novel cellulose-g-poly(acrylic acid-co-acrylamide) superabsorbent composite based on flax yarn waste. *Carbohydr. Polym.* **2012**, *87*, 2519−2525.

(44) Liang, X. Y.; Zhang, Y.; Liu, L.; Yao, J. M. Synthesis and urea-loading of an eco-friendly superabsorbent composite based on mulberry branches. *BioResources* **2013**, *8*, 130−144.

(45) Mahmoodi, N. M.; Hayati, B.; Arami, M.; Mazaheri, F. Single and binary system dye removal from colored textile wastewater by a

dendrimer as a polymeric nanoarchitecture: Equilibrium and kinetics. *J. Chem. Eng. Data* **2010**, *55*, 4660−4668.

(46) Mahmoodi, N. M.; Hayati, B.; Arami, M. Textile dye removal from single and ternary systems using date stones: Kinetic, isotherm, and thermodynamic studies. *J. Chem. Eng. Data* **2010**, *55*, 4638−4649.

(47) Wang, S. B.; Ng, C. W.; Wang, W. T.; Li, Q.; Li, L. Q. A comparative study on the adsorption of acid and reactive dyes on multiwall carbon nanotubes in single and binary dye systems. *J. Chem. Eng. Data* **2012**, *57*, 1563−1569.

(48) Gurung, M.; Adhikari, B. B.; Gao, X. P.; Alam, S.; Inoue, K. Sustainability in the metallurgical industry: Chemically modified cellulose for selective biosorption of gold from mixtures of base metals in chloride media. *Ind. Eng. Chem. Res.* **2014**, *53*, 8565−8576.

(49) Eskandarian, L.; Arami, M.; Pajootan, E. Evaluation of adsorption characteristics of multiwalled carbon nanotubes modified by a poly(propylene imine) dendrimer in single and multiple dye solutions: Isotherms, kinetics, and thermodynamics. *J. Chem. Eng. Data* **2014**, *59*, 444−454.

(50) Shi, S. X.; Pelton, R.; Fu, Q.; Yang, S. T. Comparing polymer-supported TEMPO mediators for cellulose oxidation and subsequent polyvinylamine grafting. *Ind. Eng. Chem. Res.* **2014**, *53*, 4748−4754.

(51) Ghorai, S.; Sarkar, A.; Raoufi, M.; Panda, A. B.; Schonherr, H.; Pal, S. Enhanced removal of methylene blue and methyl violet dyes from aqueous solution using a nanocomposite of hydrolyzed polyacrylamide grafted xanthan gum and incorporated nanosilica. *ACS Appl. Mater. Interfaces* **2014**, *6*, 4766−4777.

(52) Metin, A.; Ciftci, H.; Alver, E. Efficient removal of acidic dye using low-cost biocomposite beads. *Ind. Eng. Chem. Res.* **2013**, *52*, 10569−10581.

(53) Mahmoodi, N. M.; Salehi, R.; Arami, M.; Bahrami, H. Dye removal from colored textile wastewater using chitosan in binary systems. *Desalination* **2011**, *267*, 64−72.

(54) Shakeel, F.; Haq, N.; Alanazi, F. K.; Alsarra, I. A. Box-Behnken statistical design for removal of methylene blue from aqueous solution using sodium dodecyl sulfate self-microemulsifying systems. *Ind. Eng. Chem. Res.* **2014**, *53*, 1179−1188.

(55) Gong, R.; Ye, J. J.; Dai, W.; Yan, X. Y.; Hu, J.; Hu, X.; Li, S.; Huang, H. Adsorptive removal of methyl orange and methylene blue from aqueous with finger-citron-based activated carbon. *Ind. Eng. Chem. Res.* **2013**, *52*, 14297−14303.